



Study of New Granite Slab Geometries for Facade Cladding

Daisy Pinheiro^{1*}, Orlando Longo¹, Gabriel Nascimento¹ and Gilberto Couri¹

¹*Federal Fluminense University, Rua Passos da Patria 156, Niterói/RJ – 24210330, Brazil.*

Authors' contributions

This work was carried out in collaboration between all authors. Author DP designed the study and wrote the first draft of the manuscript. Author GN performed the numerical analysis. Authors OL and GC managed the literature searches. All authors read and approved the final manuscript.

Article Information

DOI: 10.9734/CJAST/2018/42824

Editor(s):

- (1) Dr. Grzegorz Golanski, Professor, Institute of Materials Engineering, Czestochowa University of Technology, Poland.
- (2) Dr. Jakub Kostecki, Professor, Faculty of Civil Engineering, Architecture and Environmental Engineering, University of Zielona Góra, Poland.
- (3) Dr. Aurora Angela Pisano, Professor, Solid and Structural Mechanics, University Mediterranea of Reggio Calabria, Italy.

Reviewers:

- (1) Giuseppe Loprencipe, Sapienza University of Rome, Italy.
 - (2) J. Dario Aristizabal-Ochoa, National University of Colombia at Medellin, Colombia.
 - (3) Charles Chinwuba Ike, Enugu State University of Science and Technology, Nigeria.
- Complete Peer review History: <http://www.sciencedomain.org/review-history/26711>

Original Research Article

Received 20 June 2018
Accepted 06 October 2018
Published 20 October 2018

ABSTRACT

Facade claddings are important for both functional and aesthetic purposes. Its design is an intricate process that encompasses science, art, and craft to resolve a myriad of problems. Claddings can influence how the property stands out in relation to its surroundings, adding aesthetic value and personality to every structure. The materials used in the facade cladding systems can be of any type. In its turn, the installation methods are adapted to the different types of materials used for the construction of the cladding system. The technical benefits of a well-designed facade-cladding project include shorter construction time, less labour requirement, and reduced maintenance cost. In Brazil, granite slabs are widely used for facade cladding. The most common pathology of stone cladding panels that cover a building is their detachment from the material they cover. In this study, new granite slab geometries are suggested to increase their adhesion (Anchorage) by interlocking the cladding plates. To verify the performance of the new geometries analyzed, simulations of their mechanical behaviour on the facade were performed by using Finite Element Analysis (FEA). The bearing capacity of traditionally utilized rectangular granite slabs was compared with "L" and "S"

*Corresponding author: E-mail: daisypinheiro@id.uff.br;

shaped slabs. The results presented a substantial increase in the carrying capacity of the cladding system, demonstrating that the proposed geometries provide increased safety against its detachment.

Keywords: *Facade cladding; granite slabs; granite slabs on facades; a direct fixation system; the finite element method.*

1. INTRODUCTION

In the twentieth century, the more pervasive use of reinforced concrete structures made stones to be used almost as a cladding material. Because of aesthetic reasons, in addition to its imposing (nobility) and the safety characteristics of the material, granite slabs lead the customer preference amongst the materials used for facade stone cladding [1]. It has been forecast that 170 million metric tons of stones will be produced globally by the year 2020 [2].

While the use of granite slabs has proven to be satisfactory in the great majority of cases and the great scientific development, granite slabs still tend to wear out over time due to a diversity of factors. For instance, exacerbated by climate and time, movements of a building's structural elements and components of its facade expand and contract, shrink and swell. Building foundations can settle unevenly, causing distortions of the structure frame. Gravity forces can shorten columns and cause the building beams and girders, to which cladding is attached, to sag slightly. Wind and earthquake loads can induce a lateral force on the building facade. Negative wind pressure can suck cladding materials off a building facade [3]. If these loads are transmitted between the structural frame and the cladding, cladding components may be subjected to forces for which they were not designed. The pathologies of granite slabs, restricted to their use in facades of buildings, are identified as surface defects: cracking, declination and detachments [4]. They are related to the geometric characteristics of the rock, especially the thickness, the connection between the rock plates, the support, the fixing methods, and the structural loads [5]. The weight of the granite slabs should be considered because the specific weight of the material is high, and since the slabs are fixed in a vertical facing, the slab weight itself contributes to increasing the risk of its detachment [6].

Several factors interfere in the degree of adhesion of granite slabs to the substrate, among them: the type of adhesive mortar

(industrialized or produced on site); the design of the project or lack thereof; lack of capacity building; climate conditions; inadequate choice of stone type; lack of knowledge of the behavior of the materials and, most importantly, the physical-mechanical characteristics of each stone and its behavior as a function of the conditions of each project [7,8,9]. The research related to the adhesion of stone cladding mostly refers to the physical-mechanical characteristics of mortars between support and claddings.

In the present study, new geometries of stone cladding slabs are proposed. The traditionally rectangular shape and new "L" and "S" shape options were analyzed and compared. The objective is twofold: Firstly, to understand their performance as a function of the differences in slab geometries. Secondly, pinpoint the geometry that provides greater security for the utilization and repair of granite slabs by the traditional anchorage method.

Brasília red granite material was chosen to perform the analyses because it is well accepted in the market and has physical-mechanical characteristics available in the literature.

2. MATERIALS CONSIDERED

2.1 Rock Strength

The strength and quality of the rock are determined by its technological properties. Its use for facade cladding requires flexural strength [10]. The weight of the stone plate, as a result of its size, will imply the adhesion strength, requiring a greater layer of support fixation, the larger the plate weight itself [11].

The mechanical strength of the rocks is characterized by the microfissural and mineralogical composition of each lithological type, where the apparent specific mass and the apparent porosity offered is indicative of physical-mechanical resistance [12]. It is also considered that, during the genesis of magmatic and metamorphic rocks, the performance of deformation mechanisms results in a varied

range of crystalline defects (punctual, linear and/or planar), which configure weakness planes or physical discontinuities of the rocks as well as the most important areas for energy redistribution and the propagation of fractures in accordance with the conceptions postulated by Griffith Theory [13] and consequent rock disintegration [14,15,16].

Brasília red granite is a rock of magmatic nature, classified as syenogranite, extracted from the municipality of Jaupacé in the Goiás state, in Brazil [17]. It has reddish colouration, thick granulation, from 0.3 mm to 5.0 cm or more, predominantly between 0.5 cm and 3.0 cm. The larger crystals are microcline, with varying shapes, which may be oval, elongated to binoculars. It has a good mineral bonding, which reflects in the cohesion of the rock. It contains 18% percent of pink feldspars, rare cream-coloured particles and greyish (felsic) quartz, 12% iron-magnesium, which materializes in crystals in shades of brown. This low ratio results in a low oxidation of the material. The presence of quartz may allow micro cracking, a vulnerable point for water absorption [18].

2.2 Fixation of Granite Plates on Facades

The most used techniques to fix granite slabs on building facades are the techniques of direct [19] and indirect anchorage [20,21]. The former is applied by bonding (physical-mechanical adhesion), with or without safety anchorage (i.e. clamps), and the latter by metallic support substructure [22].

The techniques of laying slabs using the traditional method (i.e. bonding with mortar or cement-epoxy resin) require detailed design [23].

This is to prevent the appearance of pathologies that begin as soon as the slabs settle and changes occur when they are in contact with atmosphere, pollution and cleaning products [24].

The indirect anchorage fixation process is the most efficient in the context of security, maintenance and productivity; however, when compared with the traditional system, it requires greater "careful design and a careful structural evaluation" [24].

It is a fact that small works, low jig and individual characteristics, besides the works of recovery of the facade claddings in stones, do not ignore more efficient techniques; however, they maintain and utilize methods of bonding granite slabs directly to the substrate, which requires a better performance to provide greater safety and durability [25]. The justification for that, besides the higher costs, is the lack of skilled labour and improved logistics required by the system for indirect fixation of granite slabs on facades [24].

Whatever the cladding laying technique used, the adequate result requires compliance with building procedures specific to the nature of the masonry where the stone is to be installed, the chosen anchorage method, the type of stone used, etc.

In this study, conservatively, a maximum adhesion capacity between mortar and slabs of 0.02 MPa was considered. This corresponds to a loss of 80% of the adhesion usually adopted, which is 0.1 MPa [26]. The objective of the adhesion loss is to simulate the long-term effect of fatigue on the adhesion capacity of the mortar, which is caused by the heating and cooling cycle throughout the day (transient thermal stress).

2.3 Mechanical Properties

Based on the data available in the literature, the mechanical properties required for structural analysis were studied, including specific mass, modulus of elasticity, Poisson's coefficient and maximum tensions and compression. The values of these parameters are shown in Table 1.

Table 1. Mechanical properties of materials

Property	Material				
	Masonry ¹	Gluing mortar ²	Plaster ²	Brasília red granite ³	Grout ⁴
Density (kg/m ³)	969	1900	2310	2621	2540
Young's modulus (GPa)	21.44	6.389	0.571	75	9
Poisson's coefficient	0.20	0.20	0.20	0.25	0.22
Max. tensile strength (MPa)	2.5	4.7	4.7	11.8	4
Max. compressive strength (MPa)	10	10.7	10.7	210	20

¹ Equivalent calculation for a 6-hole 10 x 16 cm brick with 1 cm of mortar between bricks; 2 [27,28,29] and [30];

³ [31,32,33,34] and [35]; 4 [27]

3. NUMERICAL MODELING

3.1 General Data

The ANSYS Mechanical version 17 [36] program was used. Its Workbench platform provides all the necessary tools for all the steps inherent to a Finite Element Analysis (FEA) in a single interface, such as: preprocessing (e.g. geometry drawing, mesh generation, and material properties definition); processing characterized by numerical calculation; and post-processing, where the analysis of the results is performed.

The simulations were performed in a three-dimensional domain and non-linear static regime, which allows the sophisticated modelling of the contact and detachment of the various components/layers that compose the cladding system. The program is based on the Finite Element Method (FEM), whose structural matrices are derived from the principle of virtual work. More details about the applied theory can be found in [36]. The mechanical properties adopted for all the materials used in this study are listed in Table 1. Further details on its formulation can be found in the theoretical manual of the program [36].

3.2 Geometry

In this study, in addition to the conventional rectangular stone cladding slab, two other shapes were proposed: the "L" and "S" shapes. All the shape dimensions are shown in Fig. 1.

The dimensions of the newly proposed cladding plate shapes (Fig. 1) were defined to ensure equivalence of area between them and, consequently, the same wind suction force in every one of them.

The geometry of the domain under study was defined, three-dimensionally, based on the thicknesses of the internal lining, masonry, plaster, bonding mortar, slabs and grout. Table 2 shows the thickness of every layer that was part of our finite element model.

Table 2. Thicknesses of components

Layer	Thickness (m)
Plate	0.03
Grout	0.03
Mortar	0.03
Plaster	0.02
Masonry	0.10
Internal coating	0.03

Cross sections were made through all layers from the perimeters of the plates to ensure compatibility for the contact between the different layers (Fig. 2).

The shaped wall is composed of five plates along the width, and five along the height, totaling 25 plates.

3.3 Domain Discretization

According to the FEA methodology, the domain was discretized into elements, as shown in Fig. 3, with the representation of an isolated plate and the underlying layers.

The shaped wall is composed of five plates along the width, and five along the height, totaling 25 plates.

3.4 Domain Discretization

According to the FEA methodology, the domain was discretized into elements, as shown in Fig. 3, with the representation of an isolated plate and the underlying layers.

For the representation of the wall layers and the plates, SOLID186 type elements were used. ANSYS' SOLID186 is a 3-D 20-node solid element of a higher order that shows quadratic displacement behaviour [36]. The element is defined by 20 nodes. Each node has three degrees of freedom (i.e. translations in the nodal x, y, and z directions). The element supports plasticity, hyper-elasticity, creep, stress stiffening, large deflection, and strain capabilities [36]. Four elements along the height and four along the width, counting 16 per plate, divided the plates. To the total, including other layers and grout, about 3,500 elements and 30,000 knots were needed to define the finite element mesh.

The pairs of contact elements CONTA174 and TARGE170, configured with the bonded option, represent the adhesion between the layers. The contact simulation occurs when the CONTA174 element surface penetrated one of the target elements (TARGE170) on a specific target surface. Each node of a CONTA174 element has three-degrees of freedom (i.e. translations in the nodal x, y, and z directions). Contact elements use the same nodes as the solid elements already defined to represent the layers. In this way, with a specific formulation, they can transfer charges or displacements from one layer to another adjacent layer. The contact pairs are limited by the maximum tension of adhesion

(traction), considered as 0.02 MPa, as previously described. In places where the calculated stress exceeds this value, the decoupling occurs

between the contact elements, which correspond in the real physical problem to the detachment (loss of anchorage).

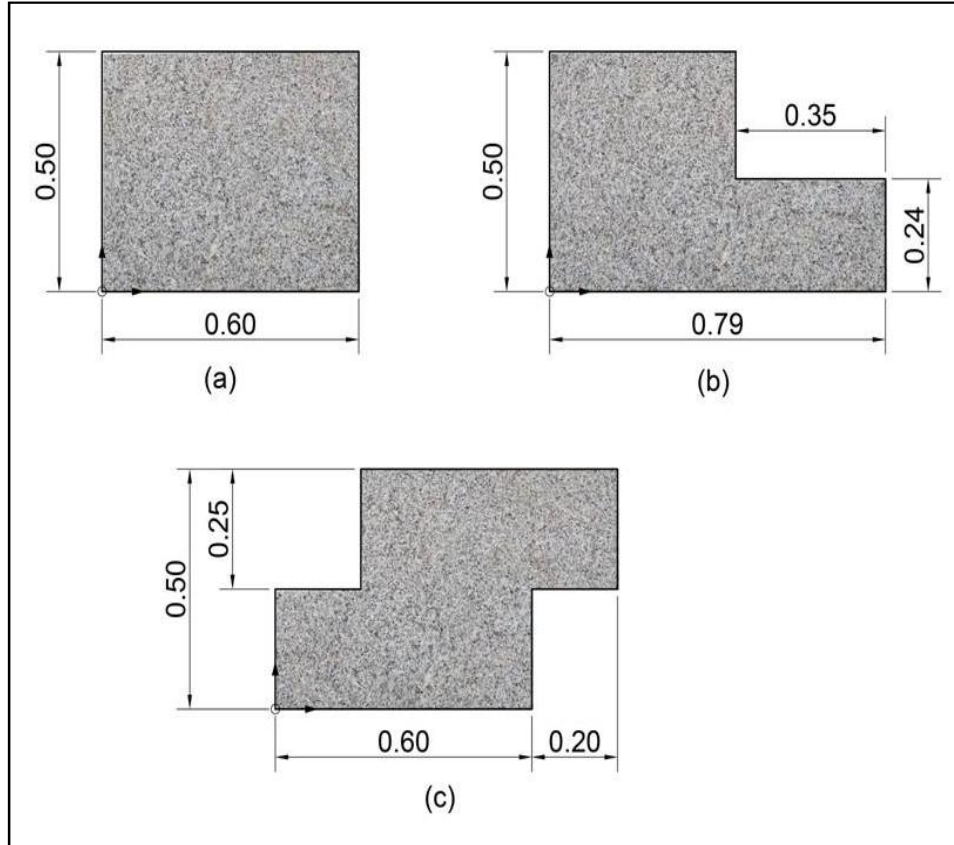


Fig. 1. Rectangular (a), "L" (b) and "S" (c) plates, with dimensions in meters

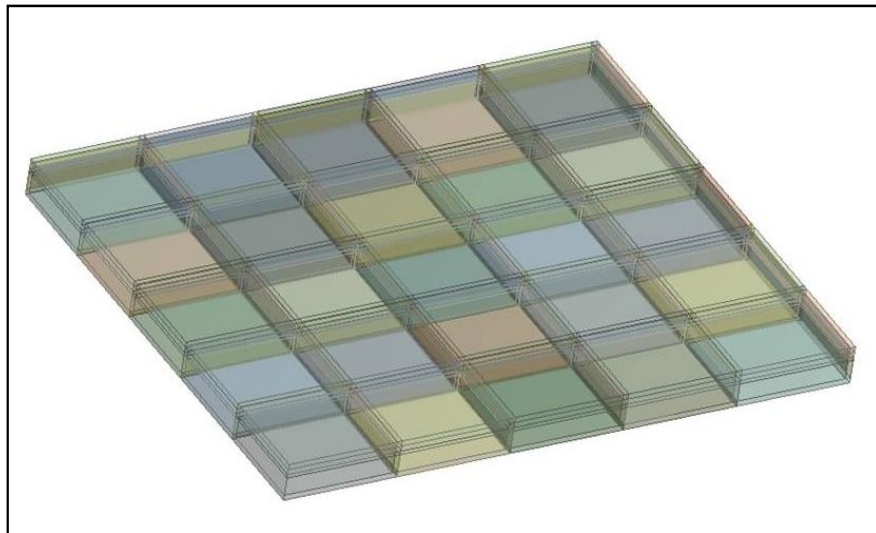


Fig. 2. Three-dimensional wall geometry (example with rectangular plates)

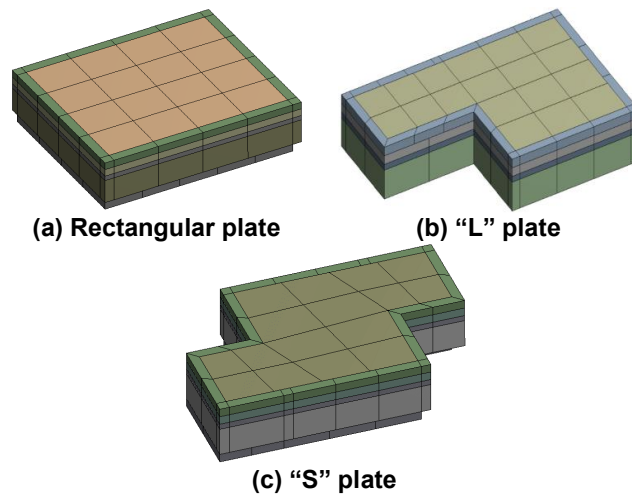


Fig. 3. Discretization of the domain in finite elements, with rectangular plates (a), in "L" (b) and in "S" (c). Representation with the stone plate and other layers

3.5 Boundary and Load Conditions

As a boundary condition, the displacements of the nodes belonging to the perimeter of the masonry layer were fixed (Fig. 4), which corresponds to the restriction imposed by more rigid structures such as pillars and beams at the ends of the wall.

To simulate a critical situation, the contact between the five central plates and the mortar was deactivated, remaining attached to the others only by the grout (Fig. 5). This scenario corresponds to the detachment of plates (failure of the adhesive mortar), which can occur due to poor execution of the work or long-term fatigue, as mentioned previously.

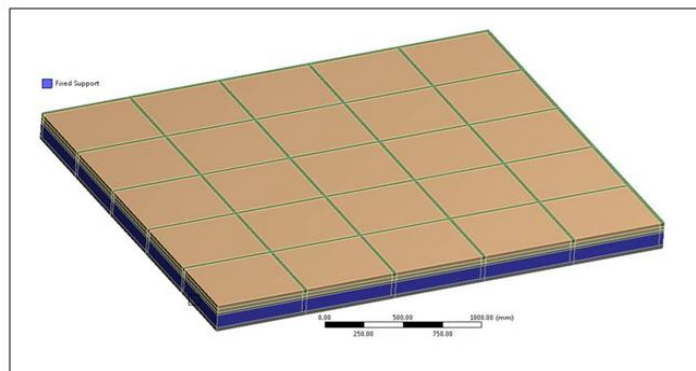


Fig. 4. Fixing the perimeter (in blue) of the mortar layer

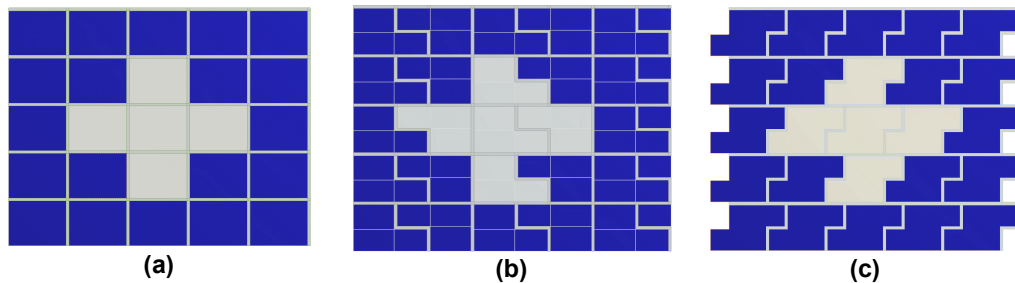


Fig. 5. Defined contact (blue area) between the mortar and the rectangular plates (a), in "L" (b) and "S" (c), with five central plates detached (gray area)

The acceleration of gravity of 9.8 m/s^2 was applied throughout the domain, which, along with the specific mass reported (Table 1), constitutes the proper weight of the structure.

A suction pressure was applied to the wall surface, which corresponds to the outer face of the plate members and the grout. The pressure value was calculated by ABNT [28]:

$$\Delta p_e = q \cdot c_{pe}, \quad (1)$$

where $c_{pe} = -1$,

$$q = 0.613 \cdot (S_1 \cdot S_2 \cdot S_3 \cdot V_0)^2 \quad (2)$$

and the parameters S_1 , S_2 and S_3 were considered as 1.00 (flat terrain), 1.13 (class A category V, $z = 10$) and 1.10 (group 1), respectively.

The defined maximum speed, V_0 is 40 m/s, was applied gradually in 80 steps. This facilitates the non-linear convergence and consequently yields more accurate results. In the first step of the simulation, the speed is zero. Thereafter, the

speed is gradually increased until the total detachment of some plate occurs when the calculation is interrupted.

4. RESULTS AND DISCUSSION

After the execution of all the simulations, which required about one hour of computational processing for each type of plate, it was possible to verify visual and numerical results through the ANSYS post-processing tool.

In Figs. 6, 7 and 8, the deformed plates calculated at the imminence of the total detachment are observed for the "L" and "S" rectangular shaped plates, respectively. The displacements were amplified by a factor of about 1,500 times, in order to facilitate the visualization and analysis of the structural behaviour.

It is observed in this set of rectangular plates that the detachment begins on the corners of the adjacent plates (Fig. 6).

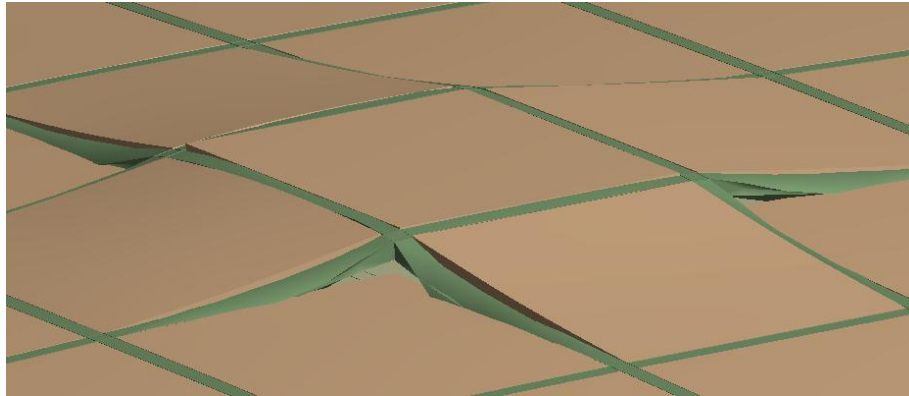


Fig. 6. Deformed rectangular plates amplified by 1500 times, imminent detachment

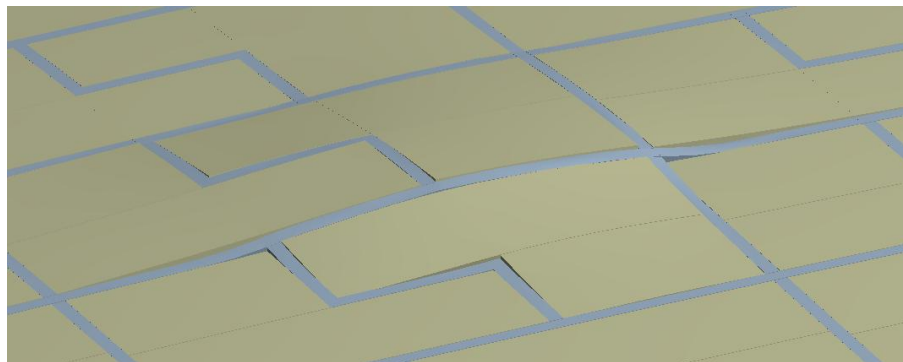


Fig. 7. Deformed L-shaped plates amplified 1,500 times, imminent detachment

In the set of "L" shaped plates, it is observed that the greatest fragility is located in the smallest corners and edges (Fig. 7). A similar behaviour occurs in the "S" plates (Fig. 8).

For both new proposed formats ("L" and "S"), an interlocking is observed, caused by the atypical geometry elaborated for this purpose, providing a greater perimeter of adhesion between adjacent plates. This effect is corroborated by the significant increase in the maximum sustained wind speed (Table 3).

Table 3. Maximum supported speeds

Plate geometry	Max. supported wind speed (m/s)
Rectangular	11.0
"L"	22.4
"S"	27.5

In addition, the stresses calculated on the plates (Fig. 9) remained much lower than the maximum allowed by granite (Table 1), which guarantees their integrity, even with the newly proposed formats.

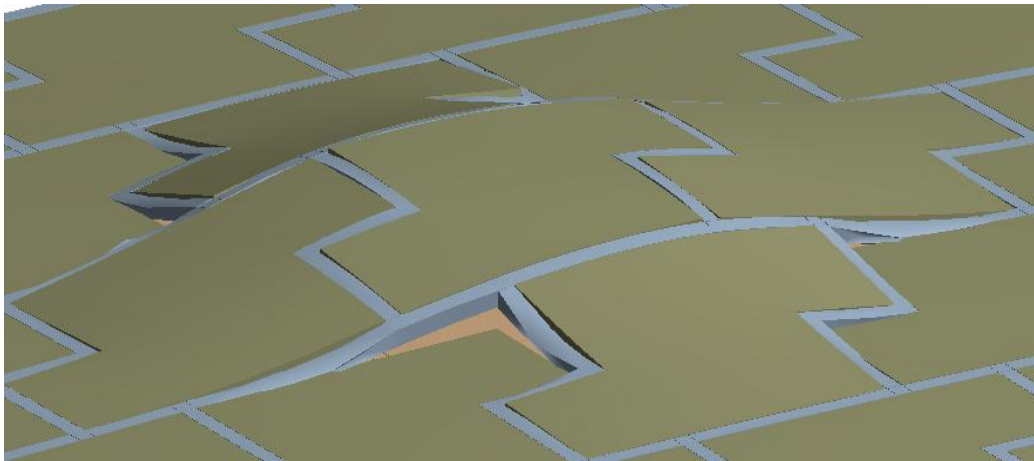


Fig. 8. Deformed "S" shaped plates amplified 1,500 times, imminent detachment

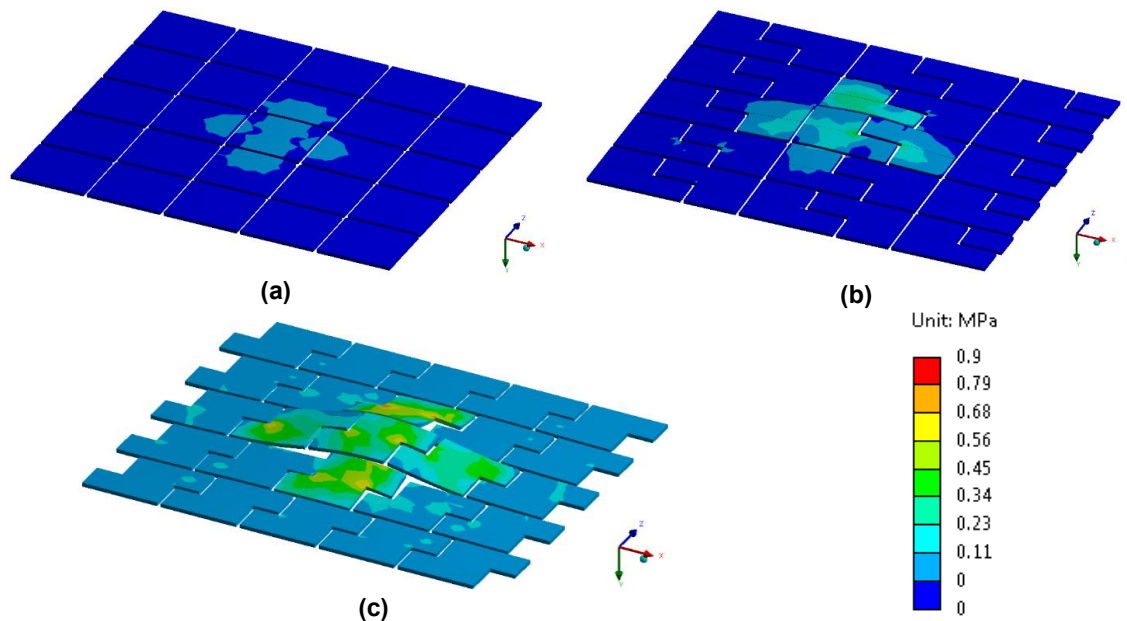


Fig. 9. Equivalent stress (MPa) calculated on rectangular shaped plates (a), in "L" (b) and in "S" (c), at the moment of impending total detachment, with deformed amplified 1,500 times

5. CONCLUSIONS

Granite slabs are widely adopted for facade cladding, and one of the most used techniques for fixing them is done through gluing mortar. The prolonged effect of fatigue causes a drastic reduction in the capacity of adhesion, which points, in many cases, as the cause of plate detachment. This paper investigated the influence of different slab geometries in adhesion resistance performance of stone cladding facades.

In order to create an interlock between plates and consequently increase the cladding system safety, the study proposed a new "L" and "S" plate geometries. To evaluate the shape effectiveness, a numerical model with adequately defined geometries, material properties, loads and boundary conditions was created.

The model simulated the bearing capacity of the slabs against a gust of wind from a scenario where there is previously a reduction of adhesion by 80%, and five plates already are detached from the mortar.

Based on the results obtained, both in graphical and numerical analyses, the following observations should be highlighted:

- In case of loss of adhesion of the slabs with the mortar at its base, the grout has the potential to serve as extra protection and to maintain the fixation by transferring forces through the perimeter of the plate.
- Both "L" and "S" plate formats exhibited a substantial increase in carrying capacity compared to the conventional rectangular shape.
- The "S" shape resulted in greater wind resistance, remaining fixed to the wall for suction pressures corresponding to wind speeds 2.5 times the value supported by rectangular plates.
- There were significant increases in the stresses on the new shape slabs. The results obtained, however, remained well below the maximum admissible values for the evaluated material (Brasília red granite), which kept its integrity.
- The numerical simulation was based on a critical scenario, with a drastic reduction of adhesion and previous detachment of five plates. However, the substantial increase in carrying capacity demonstrates that the improvement is also valid for milder and more likely scenarios.

- The applicability of the proposed shapes should still be evaluated from an economic point of view in future studies, which should also include corroboration of numerical results through experimental tests.

Finally, as a main contribution to the literature, it is concluded that the present study indicates a probable improvement of performance and safety with the proposed new geometries.

COMPETING INTERESTS

Authors have declared that no competing interests exist.

REFERENCES

1. Veiga M, Viegas J, Pinto A, Souza S, Faria J. Technical update session: The surroundings of the buildings. In II National Construction Congress. Porto, Porto: Construction Work. 2004;20-28.
2. Chiodi C. World Overview of the Ornamental and Coating Rocks Sector in 2013. São Paulo, SP: Brazilian Association of the Ornamental Rocks Industry – ABIROCHAS. 2014;1-12.
3. Brock L. Designing the exterior wall: an architectural guide to the vertical envelope. Hoboken, NJ: John Wiley; 2005.
4. Reis RS. Model for guaranteeing the quality of natural stone facing of vertical walls Master's thesis, University of Lisbon, Lisbon: Higher Technical Institute; 1992.
5. Marini P, Bellopede R. The influence of the climatic factors on the decay of marbles: an experimental study. American Journal of Environmental Sciences. 2007;3(3): 143-150.
6. Antunes M, Rosenbom K, Garcia J. Anomalies in the bonding of natural stones. I National Congress of construction mortars, APFAC, Lisbon; 2005.
7. Chiodi C. World Overview of the Ornamental and Coating Rocks Sector in 2013. São Paulo, SP: Brazilian Association of the Ornamental Rocks Industry – ABIROCHAS. 2014;1-12.
8. Gomes MF. Pathology in facades of buildings with more than five floors in the border of Maceió - AL. Specialization in Construction Planning and Technology. Maceió, AL: CESMAC; 2001.
9. Maranhão FL, Barros MMSB. Causes of pathologies and recommendations for the

- production of adherent coatings with rock plates. São Paulo: EPUSP; 2006.
10. Frascá MHB. Technological characterization of ornamental and cladding rocks: A study by means of tests and analyzes and pathologies associated to its use. In III Symposium on Ornamental Rocks of the Northeast; 2002.
11. Flain EP. Ornamental rock laying processes as a coating. In Ornamental stone laying processes as coverings, Salvador, BA: CETEM / MCTI. 2002;149-151.
12. Idemburgo K. Study of cut of ornamental rocks using diamond disk - (Master's thesis, Postgraduate Course in Metallurgical and Mining Engineering of UFMG, 2012) Belo Horizonte: Federal University of Minas Gerais; 2012.
13. Griffith AA. Theory of rupture. Proceedings of the First International Congress on Applied Mechanics, Delft. 1924;55-63.
14. Attewell PB, Farmer IW. Principles of engineering geology. London: Chapman and Hall; 1982.
15. Vutukuri VS, Lama RD, Saluja SS. Handbook on mechanical properties of rocks: testing techniques and results. Aedermannsdorf: Trans Tech Publications; 1974.
16. Whittaker BN, Singh RN, Sun G. Rock fracture mechanics: Principle, design and applications. Amsterdam: Elsevier; 1992.
17. Nogami L. Investigation of the influence of petrographic characteristics and roughness of "Granites and Marbles" plates fixed with mortar (Master's Thesis, School of Engineering, University of São Paulo, São Paulo: School of Engineering of São Carlos; 2013.
18. Silva SM, Oliveira FM, Melo EB, Pontes BM. Physical and petrographic characteristics of the Brasília and Ventura red granites and its uses in the external coating. In XXVI National Meeting of Treatment of Ores and Extractive Metallurgy, Poços de Caldas, MG. Geological Studies (UFPE). 2015;25:37-51.
19. Correia C. Pathologies identified and characterized in external facing of natural stone with direct fixation. Rocks & Equipment; 2003.
20. Gomes MF. Pathology in facades of buildings with more than five pavements in the border of Maceió - AL. Specialization in construction planning and technology. Maceió, AL: CESMAC; 2001.
21. Bauer RJF. Pathology in coating of inorganic mortar. II Brazilian Symposium on Mortars Technology. 1997;2:321-33.
22. Flain EP, Righi R, Frazão EB. Pathologies in stone-faced coatings in buildings and urban spaces in Brazil. In III Meeting of the National Association of Research and Postgraduate in Architecture and Urbanism architecture, city and project: A collective construction. São Paulo, SP: ENANPARQ; 2014.
23. Neto N, Brito J. Support system for the inspection and diagnosis of anomalies in natural stone coatings (RPN). Theory and Practice in Civil Engineering. 2011;17:9-23.
24. Moreiras ST. Methodologies for the design of "granite" slabs in non-adherent fastening systems (Doctoral dissertation, School of Engineering of São Carlos, 2014). São Carlos: USP; 2014.
DOI:10.11606/T.18.2014.tde-29052014-150736
25. Nakamura J. Facade design. Revista Técnica. 2004;92.
26. ABNT. Industrialized adhesive mortar for laying ceramic tiles: determination of tensile strength (NBR 14084) (Brazil, Brazilian Association of Technical Standards). Rio de Janeiro, RJ: ABNT; 2004.
27. Saraiva AG, Bauer E, Bezerra LM. Analysis of stresses between adhesive mortars and ceramic plates submitted to thermal stresses. In National Association of Built Environment Technology (2nd ed.), Porto Alegre: ANTAC. 2002;2:47-56.
28. ABNT. Forces due to the wind in buildings. (NBR 6123) (Brazil, Brazilian Association of Technical Standards). Rio de Janeiro, RJ: ABNT; 1998.
29. ABNT. Determination of the coefficient of linear thermal expansion. (NBR 12815) (Brazil, Brazilian Association of Technical Standards). Rio de Janeiro, RJ: ABNT; 1993.
30. Moscoso YM. Numerical and experimental study of the stresses in the adhesive mortar of facades of buildings under the action of thermo-mechanical fatigue (Master's thesis, University of Brasília, 2013). Brasília: University of Brasília; 2013.

31. Nogami N. Fixation of ornamental stone plaques: Adherence study with adhesive mortar (Master's thesis, School of Engineering of São Carlos, 2007). São Carlos: USP; 2007.
DOI:10.11606/D.18.2007.tde-07052008-085848
32. ABNT. Thermal performance of buildings. (NBR 15220) (Brazil, Brazilian Association of Technical Standards). Rio de Janeiro, RJ: ABNT; 2003.
33. Rahn PH. Engineering geology and approach. New York, NY: Prentice Hall; 1986.
34. Johnson RB, DeGraff JV. Principles of engineering geology. New York, NY: J. Wiley; 1988.
35. Goodman RE. Introduction to rock mechanics, 2nd Ed. New York, NY: J. Wiley; 1989.
36. ANSYS Inc. ANSYS Mechanical Help Release 17; 2016.

© 2018 Pinheiro et al.; This is an Open Access article distributed under the terms of the Creative Commons Attribution License (<http://creativecommons.org/licenses/by/4.0>), which permits unrestricted use, distribution, and reproduction in any medium, provided the original work is properly cited.

Peer-review history:
The peer review history for this paper can be accessed here:
<http://www.sciencedomain.org/review-history/26711>